

# PBO textile embedded in FRCM for confinement of r.c. columns

**Abstract:** Results of experimental tests on two reinforced concrete columns confined with PBO-FRCM jacketing subject to axial load and bending moments are presented, showing the effectiveness of the confinement system. Comparison of test results against theoretical results derived by a fiber model stress the ability of the confinement system to enhance both strength and deformation capacity of the confined concrete

**Keywords—** r.c. confinement, flexural ductility, FRCM, PBO fiber.

## I. Introduction

The use of Fiber Reinforced Polymer (FRP) composites as wraps or jackets for upgrading existing reinforced concrete columns has become increasingly popular in recent years [1]. This jacketing technique has been developing rapidly as it makes it possible to obtain a large increment of the deformation capacity of the concrete in critical regions [2], where large plastic deformations are expected, increase in concrete strength and reduction in loss of stiffness and strength due to cyclic action, protection and prevention of corrosion, with minimal change in the weight and geometry of the structure. However, it has been recognized that FRP confinement system has a few drawbacks: FRP cannot be applied with epoxy resin on moist elements; it has poor performance in the presence of heat and fire since the mechanical properties of the composite quickly degrade at high temperatures; moreover, the hardening phase is strongly affected by environmental temperature conditions. Thus, recently, a new fiber-reinforced composite material was developed in which epoxy resin is replaced by stabilized inorganic material (cement mortar) binding fibers with the concrete or masonry substrate [3].

The Fiber-Reinforced Cementitious Matrix (FRCM) is usually used with glass, aramidic, or carbon fiber. However, for this kind of FRCM composite, experimental results showed that the efficiency of the wrapping is limited by the connection between substrate and fiber, which is not as effective as when epoxy resins are used. To improve the performance of the

confinement system, the use of a synthetic polymeric fibre namely p-Phenylene BenzobisOxazole (PBO), was recently suggested. The molecular structure of this polymer is capable of establishing chemical bonds with hydrated compounds in a special inorganic binder by means of a hydraulic reaction. The formation of these chemical bonds between fibre and matrix helps to improve the mechanical properties of the FRCM.

In this context, results of experimental tests on two reinforced concrete columns confined with PBO fabric embedded in FRCM jacketing, subject to axial load and bending moments are presented, showing the effectiveness of the confinement system by comparing the experimental results with those obtained numerically by models that are able to reproduce the behaviour of elements with low confinement lateral pressure [4, 5].

## II. Materials and mechanical characterization

The columns were cast with a concrete typical of buildings that require structural retrofitting (low-strength concrete). Portland cement (ASTM International Type I) was used. The cement : sand : gravel proportions in the concrete mixture were roughly 1:1.9:2.33 by weight and the water/cement ratio was 0.8 in order to obtain a concrete with low compressive strength. The maximum size of the coarse aggregate was 20 mm. In order to characterize the mechanical behaviour of the concrete, for each specimen two 150mm cube specimens were prepared and tested in monotonic compression after 28 days of curing. The average compressive strength was  $R_{co}=18.98$  N/mm<sup>2</sup> and the corresponding strain  $\epsilon_{c0}=0.16\%$ , while the average ultimate strain at a residual strength of 80%  $f_{cu,80}$  was  $\epsilon_{cu,80}=0.39\%$ . Fig. 1 shows the experimental results of the four tests in terms of  $\sigma - \epsilon$  curves.

The Ruredil X Mesh Gold [6] was used a PBO fibre textile. (Fig. 2). It is a bidirectional warped mesh, with four times as many fibres in the direction of the warp as in the direction of the weft. Each equivalent textile fibre roving was 4 mm wide and the clear spacing between roving was 6 mm. The density of PBO fibres was 156 g/m<sup>3</sup>, and the equivalent textile thickness in the warp (longitudinal) direction was 0.045 mm, while in the weft (transversal) direction it was 0.012 mm. The elasticity modulus ( $E_f$ ), the tensile strength ( $f_{fu}$ ) and the ultimate value of axial strain ( $\epsilon_{fu0}$ ) of the PBO fibres in each direction were provided by the fibre manufacturer and equal to  $E_f = 270$  GPa  $E_f = 270$  GPa,  $f_{fu} = 5800$  MPa and  $\epsilon_{fu0} = 21.5$  mm/m, respectively. For the mortar, a stabilized inorganic matrix Ruredil X Mesh M750 [5] designed to connect the PBO textile with the concrete substrate was utilized. The cementitious matrix was prepared so as to obtain, after 28 days

---

Piero Colajanni, Liborio Cavaleri, Maurizio Papia  
DICAM, University of Palermo  
Italy

Marinella Fossetti  
University Kore of Enna  
Italy

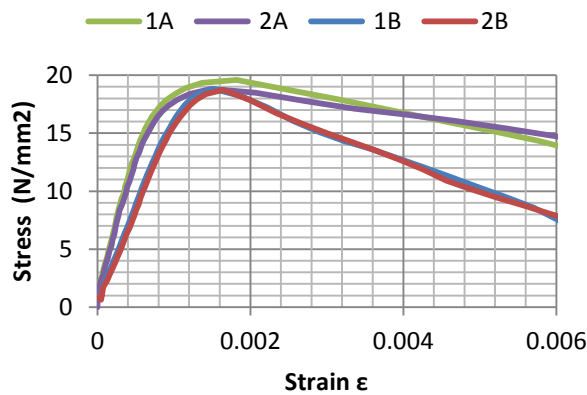


Figure 1. Stress-strain curve for unconfined concrete



Figure 2. PBO fibre textile

curing, a minimum compressive strength equal to 15 MPa, a secant modulus of elasticity equal almost to 6000 MPa and a flexural strength of minimum 2 MPa.

### III. Experimental program and test setup

The results reported here are part of a wider experimental survey aiming at evaluating the influence of cross section corner radius on the behavior of large scale r.c. columns wrapped with PBO- FRCM subjected to fixed axial load and increasing bending moment. To this aims, eight specimens with square cross-section with side  $a=200$  mm and six rectangular having sides  $a \times b=200 \times 400$  mm, half of them with cross section corner radii of 15 and the other half of 30 mm. All specimens were 1800 mm in height. Twelve specimens were wrapped with two layers of textile of height of 1000 mm, placed as to left at the two end a 400 mm height zone unwrapped; the latter choice arises from constructive restraints, and it is expected that it do not influence the behaviour of the specimen because in the unwrapped zone the bending moment will be very low. Four specimens, two for each section dimension where left unwrapped. The specimens are identified by a code in the format  $X J F\#$ , where  $X$  refers to the cross-section shape ( $X=S$  for square specimens,  $X=R$  for rectangular specimens),  $J$  refers to the corner curvature radius ( $J=15$  or  $J=30$ ), the digit  $F\#$  refers to the layer of the confinement system, for specimens confined with  $\#=2$  layers

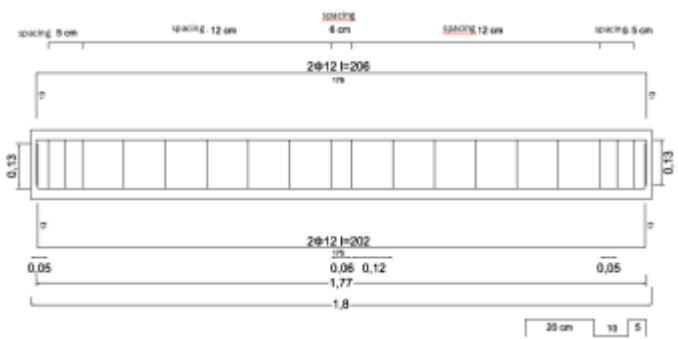


Figure 3. Longitudinal scheme of tested specimen with square section

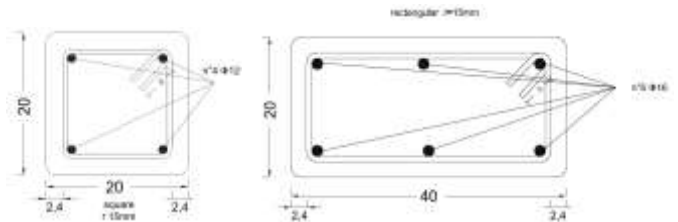


Figure 4. Cross section of specimens



Figure 5. Equipment for the imposition of the constant axial load

of textile. Square specimens were reinforced with four rebars of diameter  $\phi_1=12$  at the corner and rectangular one with six of  $\phi_1=16$  mm (Figs. 3, and 4), stirrup diameter  $\phi_w=6$  and  $\phi_w=8$  for square and rectangular specimens respectively, and stirrup spacing  $s=120$  mm. Steel grade B450C (characteristic yielding stress  $f_y=450$  Mpa) was used. Three stirrups with spacing  $s=5$  mm were placed at the support and under the load application zone. Aiming at applying a fixed axial load, at each end of the specimens, a 10 mm thick plate, an cylindrical hinge, and a 22 mm thick square plate of dimension  $400 \times 380$  mm with four holes were placed at the end of the specimens. Four S235 steel rebars with diameter  $\phi=22$  mm were inserted into the hole, parallel to the axis of the specimens (Fig. 5). On one side a load cell was inserted in order to measure the applied load during the pre-compression phase and during the whole test. The axial load were applied by a hydraulic actuator, the bolt of the rebars were screwed, the actuator were removed and the value of the applied load controlled by the load cell. Three points bending tests were performed, in order to reproduce, on the specimen parts on one side of the symmetry axis, the shape

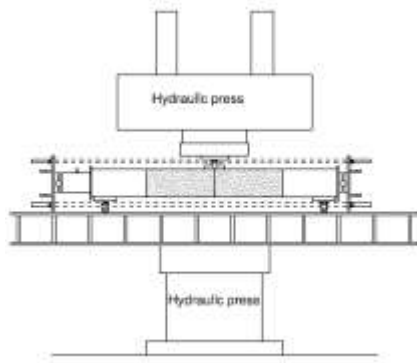


Figure 6. Test setup for three point bending test

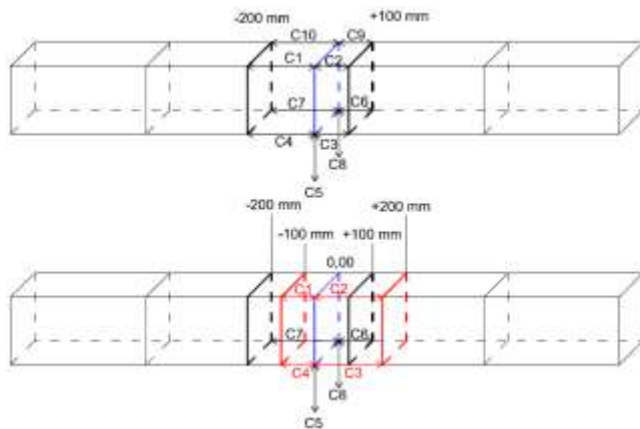


Figure 7. Electronic gauge positions for specimen Q15F2-1 and Q30F2-1

of bending moment in half columns of a shear type frame. A clear span length of 1600 mm was used. In order to perform test controlled in displacement, the specimens were tested in an hydraulic press (Zwick/Roell & Toni Technik) (Fig. 7) were the imposed displacement was regulated by an electronic control unit, user interface via personal computer and using the software TestXpert v.7.10.

At the date at which the paper is written, only two specimens were tested, namely specimens with square cross section, two layer of textile and corner radius of 15 mm (Q15F2-1, test A) and 30 mm (Q30F2-1, test B)

In Figure 7 the electronic gauges (EG) placed to measure the vertical displacement of the load application point (C5 and C8) and the axial displacement on the top and bottom chord of the beam are shown. The latter were placed to evaluate the rotation of two characteristics sections having distance equal to the half and the total height of the specimen cross section (100 mm and 200 mm) from the symmetry axis, i.e. in the region where plastic hinge rotations are expected. Two different configurations were adopted for specimen Q15F2-1 (test A), where eight EG were placed to evaluate the rotation of the two characteristic sections, and for specimen Q30F2-1 (test A), where only six EG were placed (see Figure 7).

## IV. Specimens preparation

Each specimen was firstly damped and saturated with water; then the excess water was removed. The mortar was prepared by pouring about 90% of the required amount of water into the mixer; then, the mixer started and the mortar was uninterruptedly added to prevent lumps from forming. After mixing for two to three minutes, the remaining part of the water was added and the grout was mixed for one or two more minutes. After the mix rested for two to three minutes, the grout was mixed again and applied with a smooth metal trowel in a layer about  $t_m = 3$  mm thick. After a couple of minutes, the continuous PBO textile was buried. The described procedure was repeated by interposing a layer of 3-4 mm of grout between each layer of textile. After the last layer, a 150 mm overlapping length was added To completely cover the mesh, a new mortar layer about 3 mm thick was placed all around the specimens.

## V. Behavior of confined element

In order to stress the effectiveness of the confining system, the results of experimental test are compared with the response of unwrapped and wrapped specimens evaluated by using a spread plasticity FE fiber model. To this aim, the stress-strain law for confined concrete proposed by Mander *et al* [7] are used for concrete confined by steel stirrups, and the model for concrete elements wrapped with PBO-FRCM textile proposed in [5], as a modification of the well-known model for FRP confined element proposed by Spoelstra and Monti [8] for wrapped specimens. Scott *et al.* relation for the ultimate strain are used ( $\epsilon_{cu} = 0.004 + \rho f_l / 300$ ) for both unwrapped and wrapped specimens on the basis of the estimated effective lateral confining pressure  $f_{lu}$  at the collapse.

### A. Numerical model

In Fig. 8 the stress strain curve for the stabilized inorganic mortar Ruredil X Mesh M750, the unconfined concrete, the concrete confined by the steel stirrup only, and lastly by the concrete confined by the stirrup and FRCM textile for the square specimen with corner radius  $r = 15$  mm are compared. In addition a curve is shown in which the contribute provided by the mortar, scaled by the cross section area of the mortar  $A_m$  ( $A_m = 4 t_m(a+tm)$ ) to the area of concrete  $A_c = a \times a$  ratio as done in [5] is added to the Steel+FRCM confined concrete curve. In table 1 the value of the characteristic parameters of the five curves are summarized. It is noteworthy that the confining FRCM textile ensures an increment of 24 % in both strength and ultimate strain, compared to the steel confined concrete. However it has to be emphasized that only the 19% of the strength increment is due to the confining effect, while 5% is due to mortar and vanishes when its ultimate strain is reached.

In Fig. 9 the load-deflection curves of unwrapped (steel confined) and wrapped (FRCM+steel confined) specimens (corner radius  $r_c = 30$  mm) obtained by the FEM analysis with a spread plasticity fiber model are compared. The anticipated

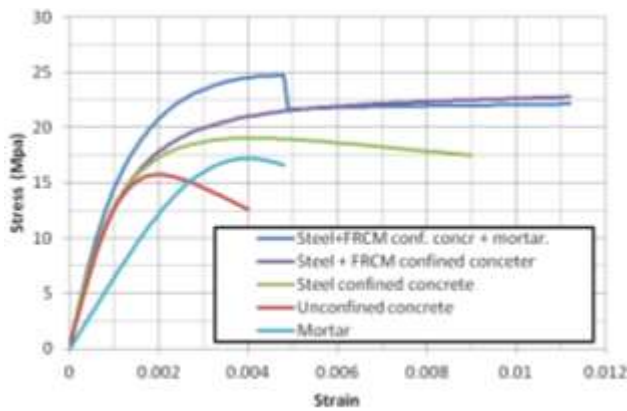


Figure 8. Analytical models: stress-strain curves of "materials"

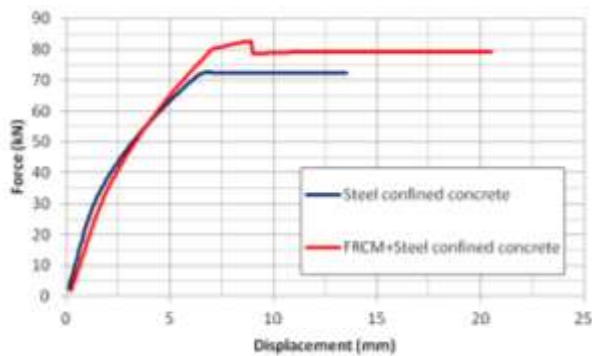


Figure 9. FE Fiber models: predicted force-deflection curves

TABLE I. MATERIAL CHARACTERISTIC PARAMETERS

Material	$f_{co}$ (Mpa)	$\epsilon_{co}$ %	$\epsilon_{cu}$ %
Organic mortar	16.1	0.23	0.40
Unconf. concrete	15.76	0.16	0.39
Steel conf. concrete	19.04	0.33	0.91
Steel+FRCM confined. concrete	22.78	1.12	1.12
Mortar+ Steel+FRCM confined. concrete	23.69	0.23	1.12

element load carrying and ultimate displacement capacity was  $F_{max,wrap} = 83.4$  kN and  $\delta_{u,wrap} = 20.52$  mm for the wrapped specimen and  $F_{max,unwrap} = 72.1$  kN and  $\delta_{u,unwrap} = 13.55$  mm for the unwrapped specimen, corresponding to an 15.6% and 51.4% assessed increment in load and displacement capacity, respectively. It has to be emphasized that in the numerical analysis of wrapped specimen the assessed value of the ultimate displacement corresponds to the inability of the software to find a solution.

## Test results

In Fig. 10 the two load vs. deflection curves obtained by the tests for the two square specimens wrapped with two layers of textile (Q15F2-1 and Q30F2-1) are reported together with the response anticipated by the FE model. In Table II, the maximum load  $F_{max}$ , the corresponding displacement  $\delta_{Fmax}$ ,

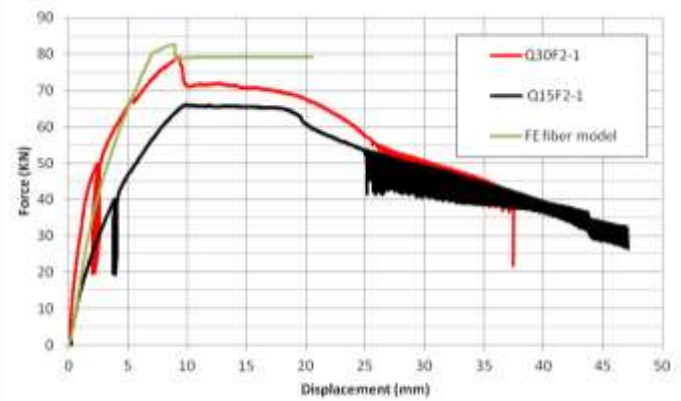


Figure 10. Fiber FE models: predicted force-deflection

TABLE II. SPECIMEN RESONSE CHARACTERISTIC PARAMETERS

Specimen	$F_{max}$ (kN)	$\delta_{FMAX}$ (mm)	$\delta_{u,80\%}$ (mm)	$\delta_y$	$\mu_\delta$
Q30F2-1	79.17	9.36	22.46	2.83	7.94
Q15F2-1	66.15	9.95	25.37	5.30	4.89
FE Fiber Model	83.4	8.83	20.52	5.1	4.02

the value of the ultimate displacement  $\delta_{u,80\%}$ , conventionally set equal to the displacement at which a residual load of 80% of  $F_{max}$ , are registered, are shown. Moreover, in order to evaluate the available displacement ductility  $\mu_d$  for the specimen, the yielding displacement  $\delta_y$  is defined as that corresponding to an elasto-perfectly plastic bi-linearization of the load vs. displacement curve, characterized by a stiffness corresponding to the secant stiffness at 60% of the maximum load of the actual curve, and an idealized strength evaluated by imposing the equality of the energy absorber by the actual and the idealized system.

The stiffness and load capacity of the curve that refers to the specimen Q30F2-1 resemble the prediction obtained by the FE fiber model, characterized by a sudden drop of the carried load when the cracking of the mortar takes action. Then, the specimen exhibits a progressive reduction of the load capacity that is typical of element confined by FRCM textile [9], and that was not captured by the FE model. The displacement corresponding to a residual load capacity of 80% is comparable to the predicted one, while the available ductility was not efficiently assessed due to an unreliable evaluation of the yielding displacement. The curve shape proves that for this axial load level ( $n=0.4$ ) the element behavior is governed by the response of the compressed concrete, and the wrapping system is able to enhance both strength and ductility of the elements. Figs. 11a and 11b show respectively the upper face and the bottom one of the specimen at the failure, attained with a wide transversal cracking in the bottom tensile chord and a small longitudinal one in the top compressed chord, due to the telescopic rupture [10] of the confining textile. The curve of the Q15F2-1 specimen exhibit stiffness and load capacity of the specimen significantly lower than the numerically predicted one, and a post peak ductile branch that



Figure 11. Q30F2-1 specimen at the test end: a) top face; b) bottom face

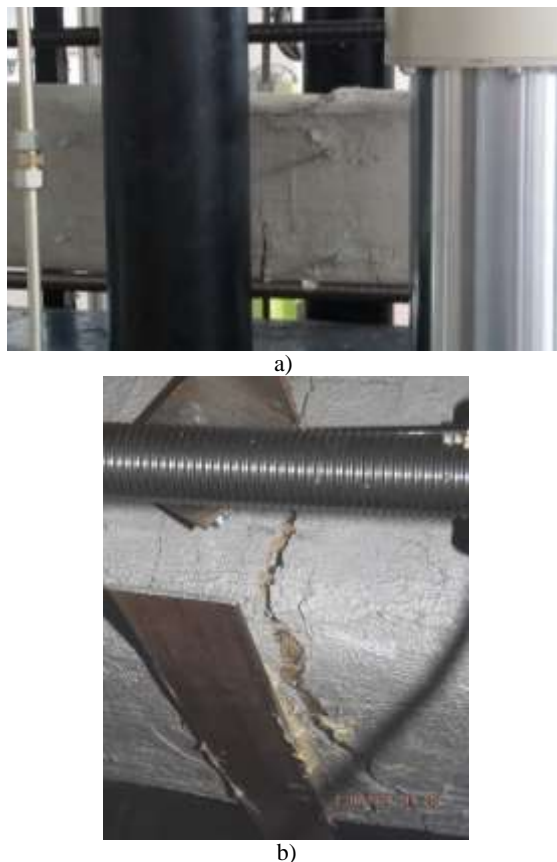


Figure 12. Q15F2-1 specimen at the failure: a) midspan section; b) bottom face

resembles the behavior of the reinforcing steel rebars; both these two circumstances can be ascribed to a level of the axial load lower than the expected one. In this condition, the confinement effect of the wrapping system is unable to increase the specimens strength, and the PBO textile is put into action only when large deflection are developed. Thus, for very large deflection the curves of the two tested specimens are similar. Figs. 12 show the collapse condition of the specimen Q15F2-1, in which the tensile PBO longitudinal fibre at the tensile bottom chord are broken, and at the compressed top chord no one apparent collapse is revealed. The small number of tested specimens and the different failure condition do not allow any consideration on the effect of the section corner radius on the behavior of wrapped specimens.

#### Acknowledgment

The Authors thanks Dr. Giovanni Mantegazza, Technical Director of RUREDIL SpA, Italy, for providing the materials for experimental test. The research was performed within the 2014-2017 Research Project “DPC–ReLUIS (Dipartimento Protezione Civile - Rete dei Laboratori Universitari di Ingegneria Sismica)”, Linea di Ricerca – Cemento Armato. The related financial support was greatly appreciated.

#### References

- [1] A. Nanni and M. Bradford. “FRP jacketed concrete under uniaxial compression”, *Construction and Building Materials*; pp. 115-124, 9(2):
- [2] G.Campione, P.Colajanni, L. La Mendola, and N. Spinella, “Ductility of Reinforced Concrete Members Externally Wrapped with Fiber-Reinforced Polymer Sheets”. *ASCE Journal of Composite for Construction*, pp. 279-290, 2007;11(3).
- [3] S.Kurtz, P. and Balaguru, “Comparison of Inorganic and Organic Matrices for Strengthening of RC Beams with Carbon Sheets”. *ASCE Journal of Structural Engineering*, 2001;127(1):35-42.
- [4] P. Colajanni, M. Papia, and N. Spinella, “Stress-Strain Law for Confined Concrete with Hardening or Softening Behavior”. *Advances in Civil Engineering*, 2013; Vol. 2013, Article ID 804904, 11 pages.
- [5] P.Colajanni, F. De Domenico, A Recupero and N. Spinella, “Concrete columns confined with fibre reinforced cementitious mortars: experimentation and modelling”, *Construction and Building Materials*, pp.375-384, Vol 52, 2014.
- [6] A. Di Tommaso, F. Focacci, G.Mantegazza, “PBO-FRCM composites to strengthen r.c. beams: mechanics of adhesion and efficiency”, *Proc. Fourth International Conference on FRP Composites in Civil Engineering (CICE 2008)*, Zurich, Switzerland, 22-24 (2008)
- [7] J. B. Mander, M. J. N. Priestley and, R. Park, “Theoretical stress-strain model for confined concrete”. *ASCE Journal of Structural Engineering*, pp. 1804-1826;114(8), 1988.
- [8] M. R. Spoelstra, and G. Monti, “FRP-confined concrete model”, *ASCE Journal of Composite for Construction*, pp. 143-150, 3(3) 1999
- [9] P. Colajanni, M. Fossetti, and G. Macaluso, “Effects of confinement level, cross-section shape and corner radius on the cyclic behavior of CFRCM confined concrete columns”, *Construction and Building Materials*, pp. 379-389 ,55, 2014.
- [10] B.Banholzer, T. Brockmann, and W. Brameshuber, “Material and bonding characteristics for dimensioning and modeling of textile reinforced concrete (TRC) elements. *Materials and Structures*, pp. 749-763,39,2006